

Microstructure and mechanical properties of sintered body of zirconia coated hydroxyapatite particles

T. MATSUNO

Kitasato University School of Medicine, 1-15-1 Kitasato, Sagami-hara, Kanagawa 228-8555, Japan

K. WATANABE, K. ONO

Nara Machinery Co., Ltd., 5-7-2 Jonan-jima, Ohta-ku, Tokyo 143-0002, Japan

M. KOISHI

Faculty of Industrial Science and Technology, Science University of Tokyo, 102-1 Tomino, Oshamanbe-cho, Yamakoshi-gun, Hokkaido 049-3514, Japan

Synthetic hydroxyapatite (HAP) has high biocompatibility and osteoconductivity [1]. The sintered body produced by pressurizing and heating the synthetic HAP particles has, however, not sufficient mechanical strength and fracture toughness [2, 3]. It is therefore, difficult to use this material as an implant material except in special cases. Meanwhile partially stabilized zirconia (PSZ) has biocompatibility and superior mechanical properties, hence it has gained attention as an implant material [4, 5]. It is, however, not expected that PSZ embedded as an artificial bone combines with a bone because it has no osteoconductivity. Several studies have been made so far to develop an artificial bone with high biocompatibility and osteoconductivity and exhibiting high mechanical properties. The results of some studies indicate that fracture toughness of the artificial bone prepared by mixing fine particles of HAP and PSZ according to a conventional method and sintering the mixture is not improved as expected due to incomplete mixing or reseparation in the mixture during the subsequent processes. It is known that HAP coexisting with PSZ is transformed to tricalcium phosphate and (or) calcium zirconium oxide at high temperature. It is also known that zirconia undergoes a phase transformation from the tetragonal system to the cubic system at high temperature in the presence of HAP [6, 7]. It is estimated that the changes are more accelerated with the decrease of the sizes of those particles. This is undesirable for the mechanical strength and osteoconductivity of the material. In consideration of the problems involved in the sintering of the mixture of HAP and PSZ particles, in this study, surface coating of relatively large-sized spherical HAP particles with small-sized PSZ particles by the dry impact blending method [8, 9] was conducted. The HAP and PSZ composite particles were sintered by hot-pressing, and the microstructure and the mechanical properties of the sintered bodies were investigated.

HAP powder (spherical particles, mean particle diameter, $9.3\text{ }\mu\text{m}$; Ca/P mole ratio, 1.67, Mitsubishi Material Co., Ltd.) and PSZ powder (mean particle diameter, $0.1\text{ }\mu\text{m}$; Y_2O_3 content, 3 mol%, Tosoh Co., Ltd.) were used. The spherical HAP particles were coated with PSZ particles using a Hybridization System

NHS-1 type (abbreviated as HYB, circumferential velocity of rotor, 60 ms^{-1} ; treating time, 3 min, Nara Machinery Co., Ltd.). The composite particles obtained were sintered by hot-pressing (argon atmosphere, 30 MPa, 1350°C , 15 min, size of sintered body, $50 \times 50 \times 7\text{ mm}^3$ or $50 \times 50 \times 16\text{ mm}^3$). Monolithic HAP sintered body was prepared by hot-pressing at 1150°C (other sintering conditions were the same as above). Bending strength was determined by four-point bending test with autograph AG-10TB of Shimadzu Co., Ltd. at a crosshead speed of 0.5 mm min^{-1} . Compressive strength was determined with autograph AG-25TB (Shimadzu) at a crosshead speed of 0.5 mm min^{-1} . Fracture toughness was measured by a single-edge V-notched beam (SEVNB) method using an autograph AG-10TB at a crosshead speed of 0.5 mm min^{-1} in three-point bending test. Modulus of elasticity was determined by an ultrasonic pulse method.

Composition of the sintered bodies prepared in this study, percentage of HAP area on the surface of these sintered bodies, and the apparatuses used for mixing or blending the HAP with PSZ, are shown in Table I. T-1 is a sintered body, which is composed only of HAP. T-2, T-4, T-5 and T-6 have been made by sintering the HAP/PSZ composite particles prepared by HYB. T-3 has been made by sintering the HAP/PSZ power mixture prepared by using a conventional powder mixer with rotary vanes (O.M. Dizer; it is abbreviated as OM). Percentage of HAP area in Table I means percentage of HAP area to total area of the sintered body surface. When this value is too small, such case is undesirable, because osteoconductivity might be poor. Densities of HAP and PSZ are 3.16 g cm^{-3} and 6.05 g cm^{-3} , respectively. Since density of PSZ is almost 2 times of that of HAP, even when weight ratio of HAP/PSZ becomes 1/2 (T-6), about half of total area on the sintered body surface is occupied by HAP. The size distribution of HAP used is shown in Fig. 1. Value shown on an axis of abscissas is volume percentage. Because no difference is observed depending on a difference of particle diameter in the case of HAP used in this experiment, volume percentage has the same value of weight percentage. Although HAP particles with a particle diameter less than $1\text{ }\mu\text{m}$ exist as well, around 80% of HAP particles

TABLE I Sintered bodies prepared in this study

Sample	HAP/PSZ			The percent of	
	Mole ratio	Weight ratio	Volume ratio	HAP area (%)	Apparatus
T-1	1/0	1/0	1/0	100	—
T-2	1/5.22	1/0.64	1/0.34	75	HYB ^a
T-3	1/5.22	1/0.64	1/0.34	75	OM ^b
T-4	1/8.15	1/1.00	1/0.52	66	HYB
T-5	1/12.24	1/1.50	1/0.78	56	HYB
T-6	1/16.31	1/2.00	1/1.04	49	HYB

^aHybridization system.

^bO.M. Dizer.

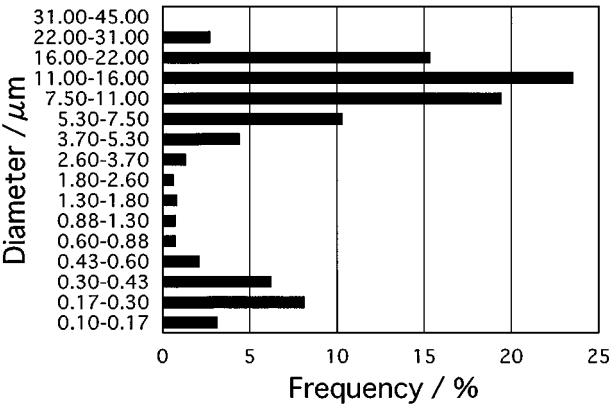


Figure 1 Particle size distribution of the spherical HAP.

have a particle diameter above 20 times of that of PSZ particles, namely more than $2\text{ }\mu\text{m}$. Micropores with a diameter of some $0.5\text{ }\mu\text{m}$ are densely distributed on the entire surface of HAP particles, and therefore it was inferred that these PSZ particles would get into them, in the case of blending the HAP particles with the PSZ.

An illustration for HAP/PSZ composite particles is shown in Fig. 2. In the case of these composite particles, the surface of HAP particles is completely coated with PSZ particles. Accordingly, the HAP particles themselves do not contact each other inside the HAP/PSZ composite sintered bodies, and therefore it is expected that three dimensional mesh structure of PSZ excellent in mechanical strength will be constructed. In a cross section of T-4, mapping results of Ca and Zr obtained by EDS are shown in Fig. 3. Fig. 3a shows the mapping

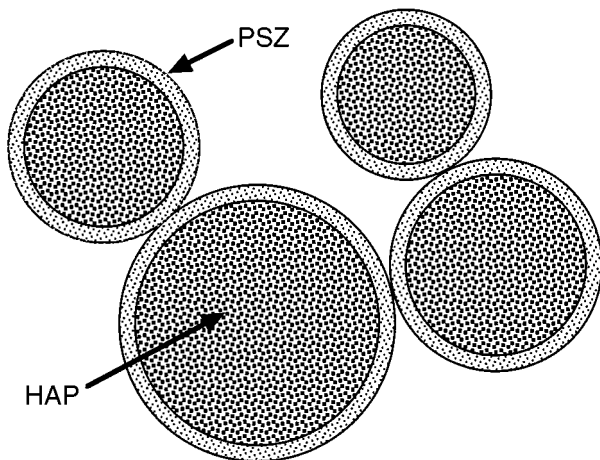


Figure 2 Illustration for HAP/PSZ composite particles prepared by HYB.

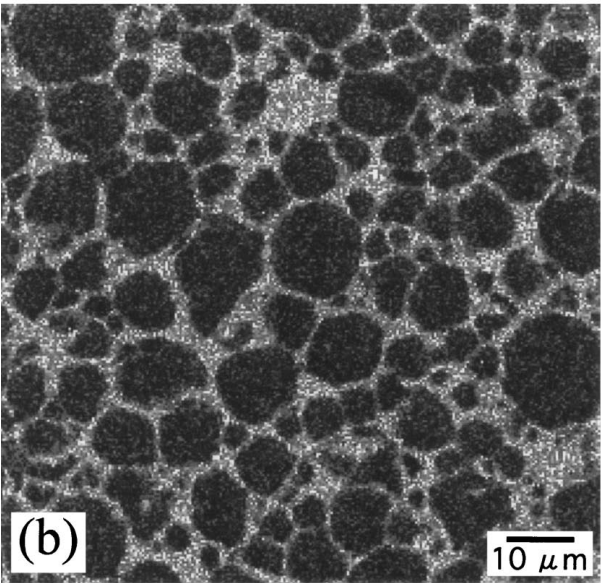
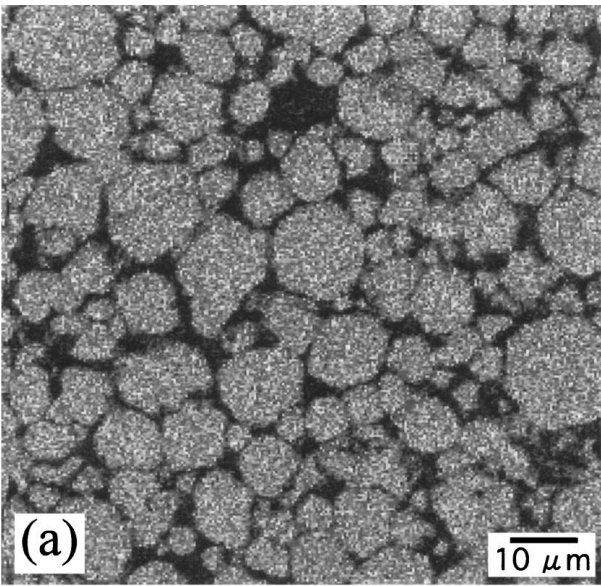


Figure 3 EDS analysis on a cross section of T-4 showing the mapping of (a) Ca ($\text{Ca-K}\alpha$) and (b) Zr ($\text{Zr-L}\beta$).

of Ca and it represents the position of HAP. Fig. 3b is the mapping of Zr presenting the location of PSZ. It shows that three dimensional mesh structure exists inside the HAP/PSZ composite sintered bodies, and furthermore the HAP particles were separate without contacting each other in these sintered bodies. In the case of HAP/PSZ composite sintered bodies of this study, any chemical change in both has not been recognized

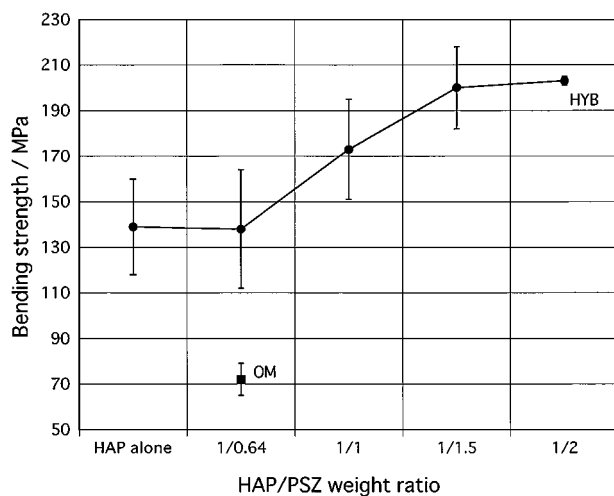


Figure 4 Relationship between bending strength of the sintered body and HAP/PSZ weight ratio.

using an X-ray diffraction method. As a cause of these phenomena, it is considered that crystallinity of HAP particles were high, a particle diameter was large, and on top of those the retention time at the highest temperature was short because sintering was performed using a hot-pressing. Bending strengths of the sintered bodies are shown in Fig. 4. As compared with that bending strength of T-1 is 139 MPa, bending strength of T-2 is 138 MPa, and thereupon no significant change is observed between them. In the case of T-4, bending strength was raised up to 173 MPa, and furthermore in the case of T-5, it arrived at 200 MPa. In contrast to it, bending strength of T-3 was 72 MPa, and in consequence a remarkable difference has been recognized between sintered bodies made by HYB and a sintered body made by OM. A SEM image at a cross section of specimen T-4 after a bending test is shown in Fig. 5. Domains appearing to be black are HAP, and that which seemed to be whitish mesh is PSZ phase. Every HAP particle has been fractured, and moreover no HAP particle dropped out from PSZ phase during fracturing, was observed. It means that the HAP particles and PSZ phase combine tightly together. There were innumerable

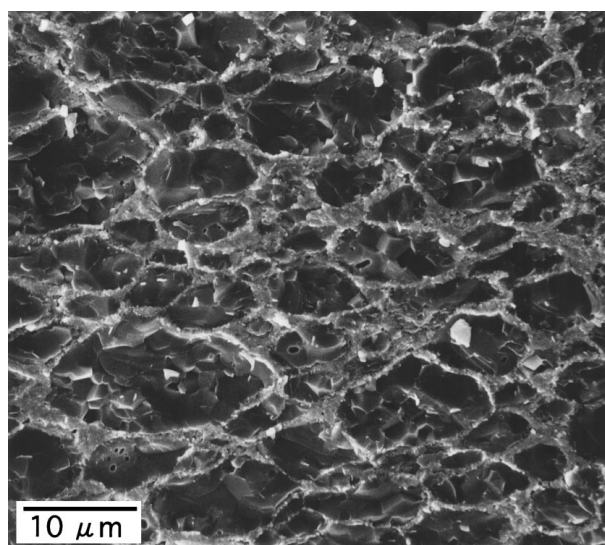


Figure 5 SEM image at a cross section of T-4 after a bending test.

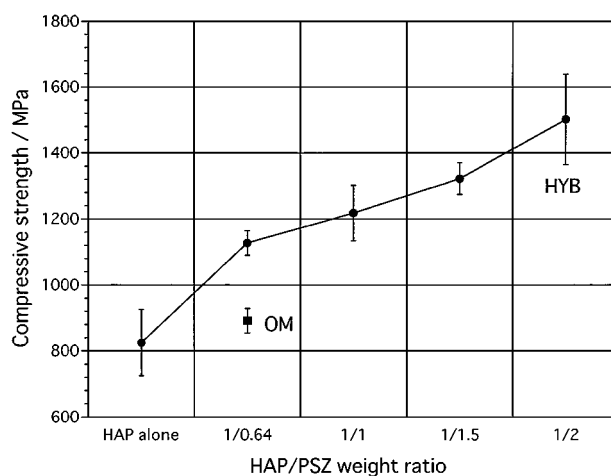


Figure 6 Relationship between compressive strength of the sintered body and HAP/PSZ weight ratio.

able micropores with a diameter of about $0.5 \mu\text{m}$ on the surface of HAP particles as mentioned before. It was guessed that the PSZ phase had come into these pores and consequently the HAP particles and PSZ phase combined tightly through so called mechanical coupling. As shown in Fig. 5, a fractured surface of the HAP particles appears to be relatively flat, whereas a great number of fine unevenness is observed on the surface of PSZ phase. These facts strongly suggest that bending strength of the HAP/PSZ composite sintered body depends on the PSZ phase.

Compressive strengths of the sintered bodies are shown in Fig. 6. In the case of T-1, compressive strength was 825 MPa, but in the case of T-2, it increased to 1127 MPa, and thereafter also it became larger as an increase of PSZ contents, and furthermore in the case of T-6, it reached 1501 MPa at last. In the case of the HAP/PSZ powder mixture prepared by OM, compressive strength of a sintered body T-3 was 891 MPa, and accordingly it was significantly smaller than those of the case for HYB. PSZ contents of the HAP/PSZ composite sintered bodies substantially affect their fracture toughness (Fig. 7). For example, in the case of T-2, its fracture toughness was 2.9 times of that of

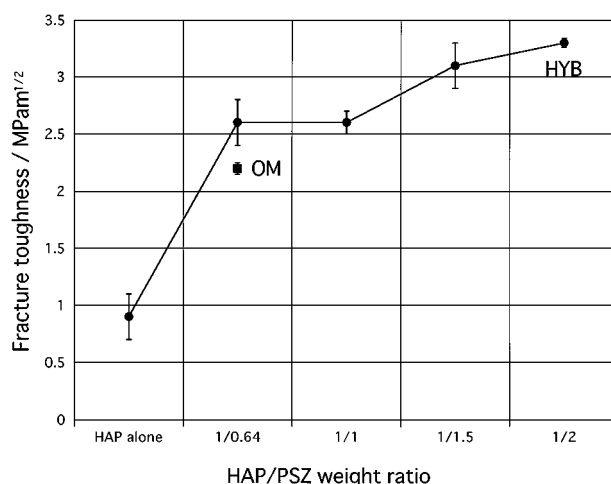


Figure 7 Relationship between fracture toughness of the sintered body and HAP/PSZ weight ratio.

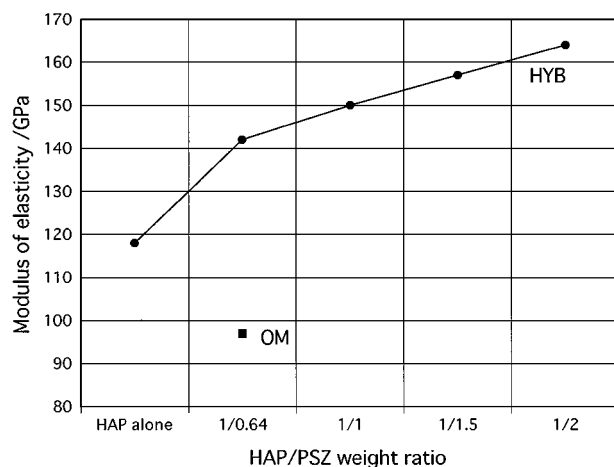


Figure 8 Relationship between modulus of elasticity of the sintered body and HAP/PSZ weight ratio.

T-1. Fracture toughness of the sintered bodies increased along with an increase of PSZ contents, and in the case of T-6, it has attained $3.3 \text{ MPa m}^{1/2}$. With respect to fracture toughness as well, T-3 showed smaller value than T-2. Also with regard to modulus of elasticity, a similar tendency to other mechanical properties was observed, and its value increased in concert with an increase of PSZ contents (Fig. 8). In the case of T-3, its value of modulus of elasticity was smaller than that of T-1. There are several existing reports with reference to mechanical strength of human compact bone, and it is well known that bending strength is 50–150 MPa, compressive strength is 100–230 MPa, fracture toughness is $2\text{--}6 \text{ MPa m}^{1/2}$, and modulus of elasticity is 7–30 GPa. Mechanical strength of the HAP/PSZ composite sintered bodies acquired in this experiment is not only

superior to that of a sintered body composed only of HAP, but also is on the same par or larger in comparison with mechanical strength of human compact bone. In the case of the HAP/PSZ composite sintered bodies obtained in this study, their fracture toughness is especially superior to that of other bioactive ceramics by far, and therefore their utilization as the substitute material for human compact bone can be well considered. By using this material, there is a fair chance for expanding the range of curative treatment to those people who have lost their bone by a disease or injury. Osteoconductivity of this material has been under investigation, and its favorable results will be reported later.

References

1. K. ONO, T. YAMAMURO, T. NAKAMURA and T. KOKUBO, *Biomaterials* **11** (1990) 265.
2. J. D. SANTOS, P. L. SILVA, J. C. KNOWLES, S. TALAL and F. MONTEIRO, *J. Mater. Sci. Mater. Med.* **7** (1996) 187.
3. P. E. WANG and T. K. CHAKI, *ibid.* **4** (1993) 150.
4. K. SHIRAIISHI and H. FUJIKI, *Orthopaedic Ceramic Implants* **3** (1983) 81.
5. P. KUMAR, M. OKA, K. IKEUCHI, K. SHIMIZU, T. YAMAMURO, H. OKUMURA and Y. KOTOURA, *J. Biomed. Mater. Res.* **25** (1991) 813.
6. K. IOKU, S. SOMIYA and M. YOSHIMURA, *J. Ceram. Soc. Japan* **99** (1991) 196.
7. Y. YAMADA and R. WATANABE, *ibid.* **103** (1995) 1264.
8. H. HONDA, M. KIMURA, T. MATSUNO and M. KOISHI, *Chimicaoggi* **9** (1991) 21.
9. H. HONDA, M. KIMURA, F. HONDA, T. MATSUNO and M. KOISHI, *Colloids Surfaces A: Physicochem. Eng. Aspects* **82** (1994) 117.

Received 27 August
and accepted 18 October 1999